Electronic Supplementary Material (ESI) for Inorganic Chemistry Frontiers.

Supporting Information for

Squaramide-based Anionic Hydrogen-Bonded Organic Framework: Enhancing Sensing Performance for Pesticides by Post-Metallization with *In situ* Imaging

Weiwei Jiang,[a] Hao Zheng,[a] Yuxuan Wu,[a] Pengyan Wu,*[a] Liyuan Jing,[a] Xingcheng Yuan,*[a] Xichen Wang[a] and Jian Wang*[a]

[a] Jiangsu Key Laboratory of Green Synthetic Chemistry for Functional Materials, School of Chemistry and Materials Science, Jiangsu Normal University, Xuzhou, 221116, P. R. China.

Materials and Methods:

All reagents and solvents in this work were of reagent grade and obtained commercially without further purification. 5,5'-((3,4-dioxocyclobut-1-ene-1,2-diyl)bis (azanediyl))diisophthalic acid (H_4DBDA) was synthesized according to the published procedure (*Chem. Commun.,* 2016, *52*, 8585). $Eu(NO_3)_3 \cdot 6H_2O$ was purchased from Alfa Aesar. 2,6-dichloro-4-nitroaniline (DCN), *m*-nitrotoluene (*m*-NT), nitrobenzene (NB), aniline (A), phenol, chlorobenzene (CB), 2,4-dinitrotoluene (DNT), *p*-nitroaniline (*p*-NA), *o*-nitroaniline (*o*-NA), *m*-nitroaniline (*m*-NA), 3-nitropropionic acid (3-NPA), 1-chloro-3-nitrobenzene (CN), hexaconazole (HCZ), triclosan (TCS), 2,4-dichlorophenol (DCP), isoproturon (IPU) and diuron (DCMU) were provided from Shanghai Fourth Chemical Reagent Company (China). Stock solution (2×10^{-2} M) of the ethanol solution DCN was prepared for further experiments.

Instruments and spectroscopic measurements:

The elemental analyses of C, H and N were performed on a Vario EL III elemental analyzer. X-Ray powder diffraction (XRD) patterns was recorded on a Rigaku D/max-2400 X−ray powder diffractometer (Japan) using Cu-*K*α (λ = 1.5405 Å) radiation. X-ray photoelectron spectroscopy (XPS) experiments were performed with a PHI QUANTUM2000 surface analysis instrument. The morphologies of the prepared samples were recorded by a Field Emission Scanning Electron Microscopy (SEM) of Hitachi SU8010. Samples were treated *via* Pt sputtering for 90 s before observation. FT−IR spectra were recorded as KBr pellets on JASCO FT/IR−430. Thermogravimetric analysis (TGA) was carried out at a ramp rate of 5 °C/min in a

nitrogen flow with a Mettler-Toledo TGA/SDTA851 instrument. Uv-*vis* spectra were measured on a JASCO V-530 spectrometer. Fluorescence spectra of the solution were obtained using the FP6500 spectrometer (JASCO). Both excitation and emission slit widths were 2.5 nm. Fluorescence measurements were carried out in a 1 cm quartzcuvette with stirring the suspension of Eu@DBDA.

Crystal data of DBDA:

$C_{24}H_{26}N_4O_{10}$, Mr = 530.49, Triclinic, space group P-1, a = 8.713(2), b = 10.146(2), c = 14.257(3) Å, α = 91.183(3), β = 104.081(3), γ = 101.059(3), V = 1196.8(4) Å^3, Z = 2, Dc = 1.472 g cm^{-3}, μ(Mo−Kα) = 0.116 mm^{-1}, T = 296(2) K. 2026 unique reflections [R_{int} = 0.0215]. Final R_1[with I > 2σ(I)] = 0.0419, wR_2(all data) = 0.1106, GOOF = 1.021. CCDC number: 2206854.

Crystallography:

Intensities were collected on a Bruker SMART APEX CCD diffractometer with graphitemonochromated Mo-Kα (λ = 0.71073 Å) using the SMART and SAINT programs. The structure was solved by direct methods and refined on F^2 by full-matrix least-squares methods with SHELXTL *version* 5.1. Non-hydrogen atoms of the ligand backbones were refined anisotropically. Hydrogen atoms within the ligand backbones were fixed geometrically at calculated positions and allowed to ride on the parent non-hydrogen atoms.

Table S1. Selective bond distance (Å) and angle (°) in DBDA.

O(1)−C(52)	1.279(4)	O(2)−C(58)	1.284(5)
O(3)−C(58)	1.226(5)	O(4)−C(52)	1.234(4)
O(5)−C(50)	1.220(4)	O(6)−C(68)	1.229(4)
O(14)−C(81)	1.288(5)	O(15)−C(81)	1.230(4)
O(18)−C(83)	1.253(4)	O(20)−C(83)	1.245(5)
N(1)−C(57)	1.325(5)	N(1)−C(34)	1.416(4)
N(2)−C(36)	1.339(5)	N(2)−C(55)	1.417(4)
C(7)−C(40)	1.382(5)	C(7)−C(33)	1.388(5)
C(7)−C(83)	1.510(5)	C(10)−C(39)	1.379(5)
C(10)−C(35)	1.379(5)	C(10)−C(81)	1.480(5)
C(12)−C(55)	1.390(5)	C(12)−C(15)	1.392(5)
C(15)−C(35)	1.385(5)	C(15)−C(52)	1.491(5)
C(30)−C(33)	1.380(5)	C(30)−C(46)	1.383(5)
C(30)−C(58)	1.489(5)	C(34)−C(46)	1.380(5)
C(34)−C(40)	1.381(5)	C(36)−C(57)	1.415(5)
C(36)−C(50)	1.484(6)	C(39)−C(55)	1.373(5)
C(50)−C(68)	1.456(6)	C(57)−C(68)	1.452(6)
C(71)−N(4)	1.471(5)	N(4)−C(73)	1.458(5)
C(90)−N(3)	1.454(5)	N(3)−C(79)	1.443(6)
C(57)−N(1)−C(34)	125.5(3)	C(36)−N(2)−C(55)	126.6(3)
C(40)−C(7)−C(33)	118.2(4)	C(40)−C(7)−C(83)	122.2(4)
C(33)−C(7)−C(83)	119.7(4)	C(39)−C(10)−C(35)	119.6(4)
C(39)−C(10)−C(81)	119.8(4)	C(35)−C(10)−C(81)	120.6(4)
C(55)−C(12)−C(15)	120.8(4)	C(35)−C(15)−C(12)	118.6(4)
C(35)−C(15)−C(52)	118.2(4)	C(12)−C(15)−C(52)	123.2(4)
C(33)−C(30)−C(46)	119.3(4)	C(33)−C(30)−C(58)	119.9(4)
C(46)−C(30)−C(58)	120.8(4)	C(30)−C(33)−C(7)	121.2(4)
C(46)−C(34)−C(40)	119.2(4)	C(46)−C(34)−N(1)	121.3(4)

C(40)−C(34)−N(1)	119.4(4)	C(10)−C(35)−C(15)	120.9(4)
N(2)−C(36)−C(57)	130.6(4)	N(2)−C(36)−C(50)	139.2(4)
C(57)−C(36)−C(50)	90.2(3)	C(55)−C(39)−C(10)	120.9(4)
C(34)−C(40)−C(7)	121.5(4)	C(34)−C(46)−C(30)	120.5(4)
O(5)−C(50)−C(68)	133.7(4)	O(5)−C(50)−C(36)	137.7(4)
C(68)−C(50)−C(36)	88.6(3)	O(4)−C(52)−O(1)	123.7(4)
O(4)−C(52)−C(15)	120.6(4)	O(1)−C(52)−C(15)	115.7(4)
C(39)−C(55)−C(12)	119.1(3)	C(39)−C(55)−N(2)	122.6(4)
C(12)−C(55)−N(2)	118.2(4)	N(1)−C(57)−C(36)	133.2(4)
N(1)−C(57)−C(68)	135.3(4)	C(36)−C(57)−C(68)	91.4(3)
O(3)−C(58)−O(2)	122.7(4)	O(3)−C(58)−C(30)	119.4(4)
O(2)−C(58)−C(30)	117.9(4)	O(6)−C(68)−C(57)	136.2(4)
O(6)−C(68)−C(50)	133.9(4)	C(57)−C(68)−C(50)	89.8(3)
O(15)−C(81)−O(14)	123.3(4)	O(15)−C(81)−C(10)	120.0(4)
O(14)−C(81)−C(10)	116.7(4)	O(20)−C(83)−O(18)	124.1(4)
O(20)−C(83)−C(7)	118.3(4)	O(18)−C(83)−C(7)	117.6(4)
C(73)−N(4)−C(71)	114.2(4)	C(79)−N(3)−C(90)	113.5(4)

Figure S1. View of the asymmetric unit of DBDA.

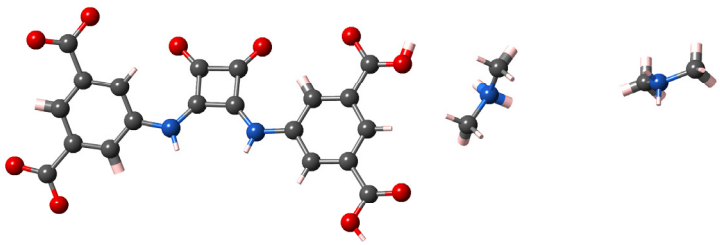

Figure S2 The view of the packing structure of DBDA along *a* direction and *b* direction.

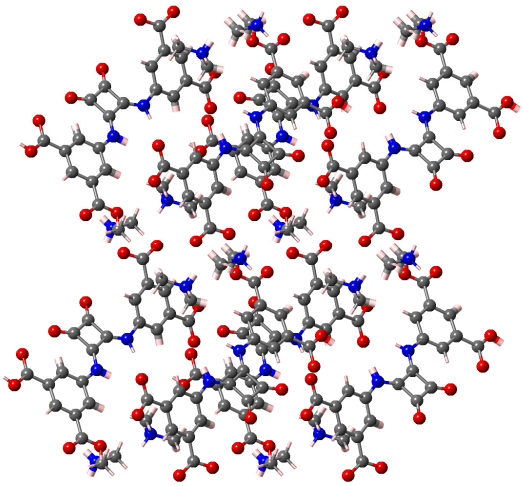

a axis

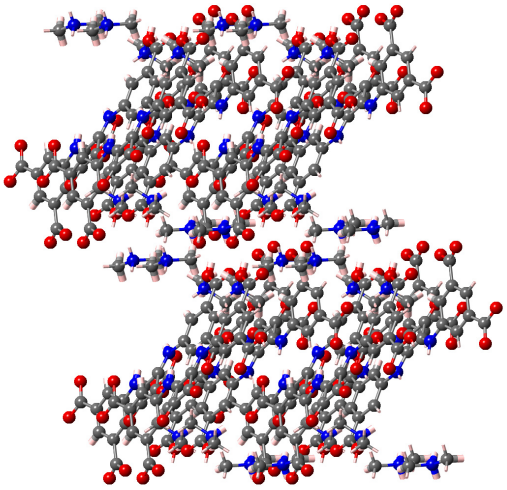

b axis

Figure S3. TGA traces of DBDA and Eu@DBDA ranging from room temperature to 800 °C.

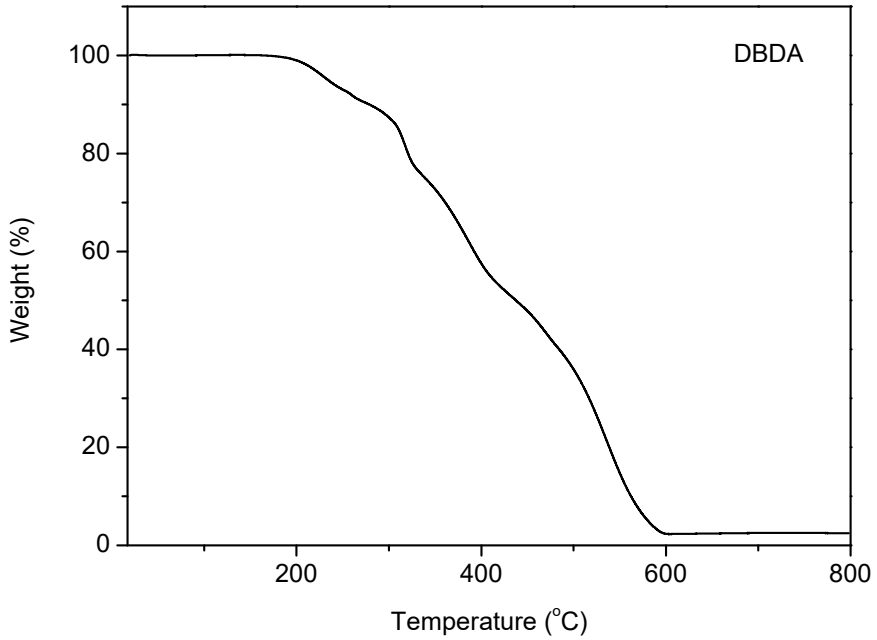

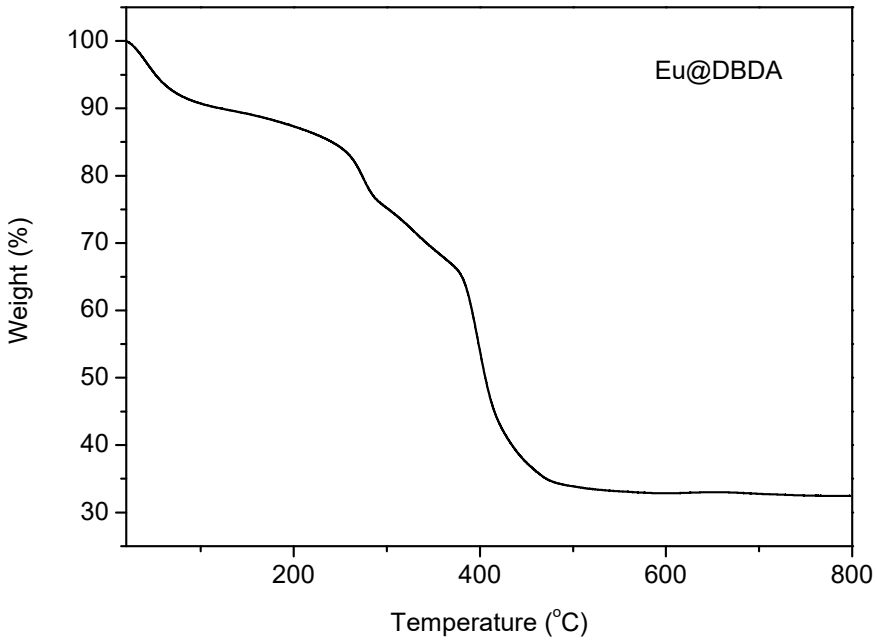

Figure S4. Luminescence spectra of DBDA (black) and Eu@DBDA (red).

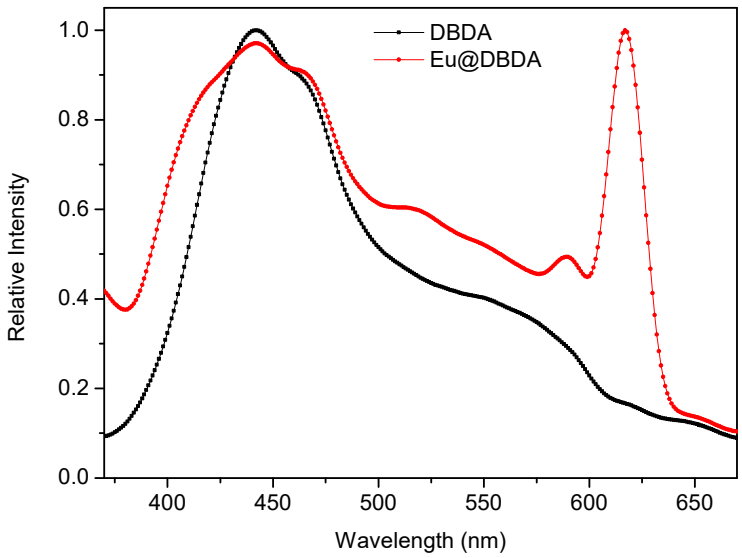

Figure S5. Families of various fluorescence spectra of Eu@DBDA in ethanol solution upon the addition of 0.38 mM of different selected analytes.

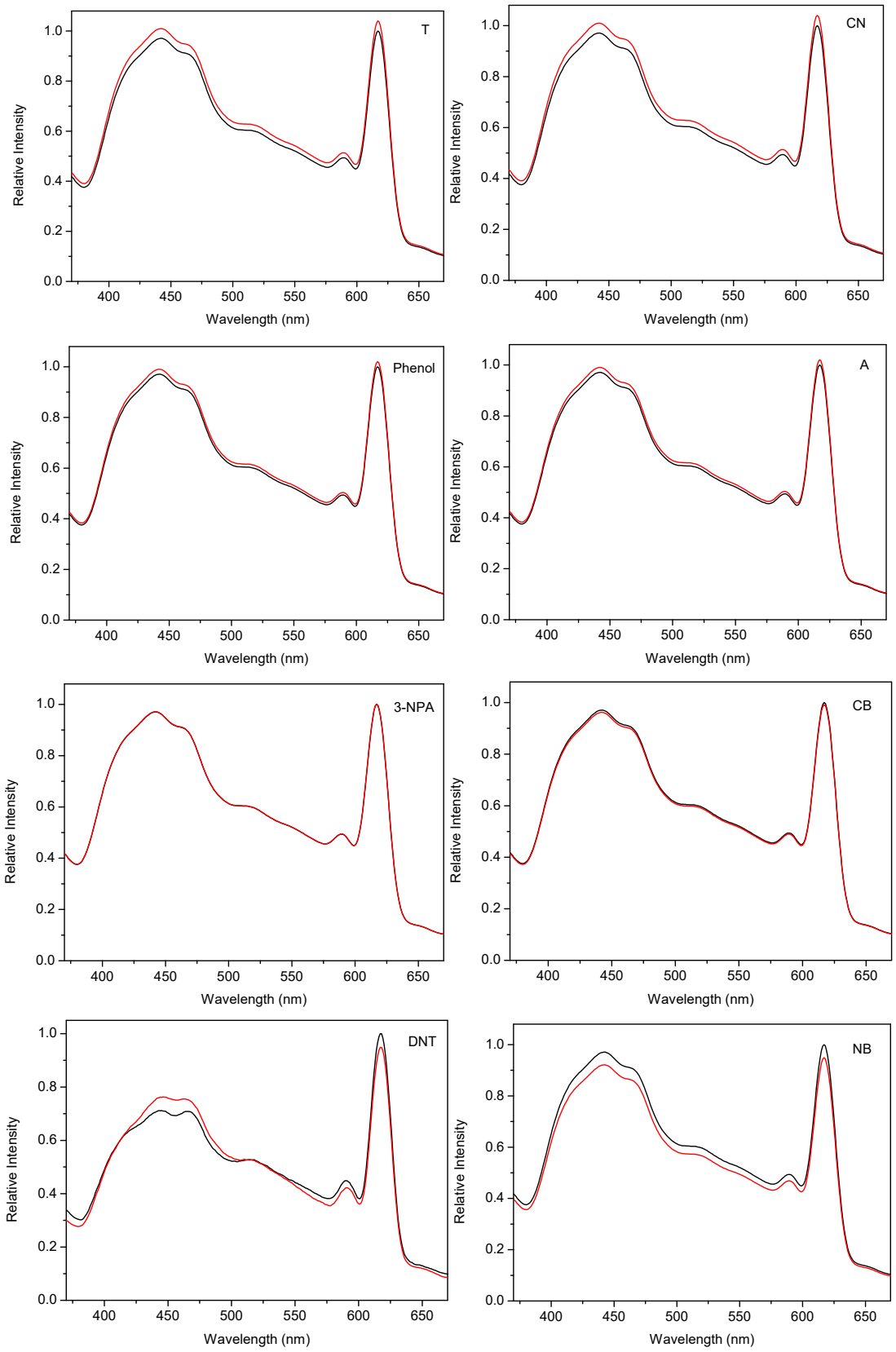

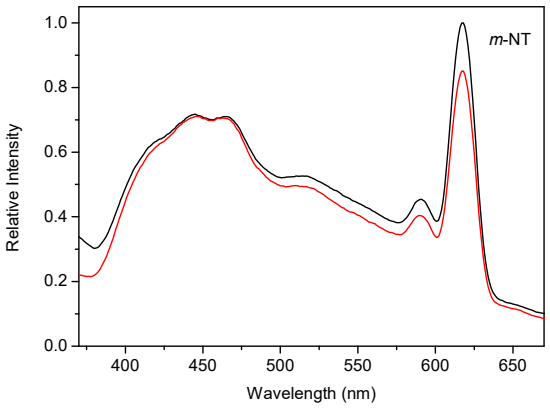
1.0
0.8
0.6
0.4
0.2
0.0
Relative Intensity
400
450
500
550
600
650
Wavelength (nm)
m-NT

Figure S6. XPS spectra of DBDA and Eu@DBDA.

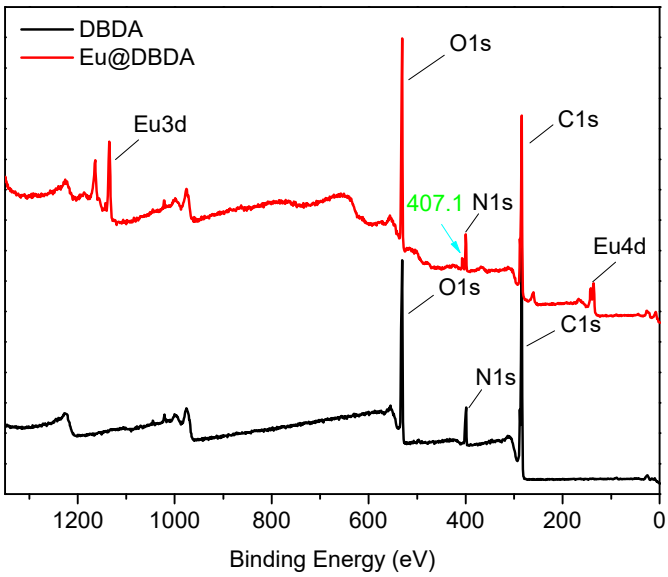

Figure S7. The fluorescence titration data of an EtOH solution of *p*-NA to the suspension of Eu@DBDA.

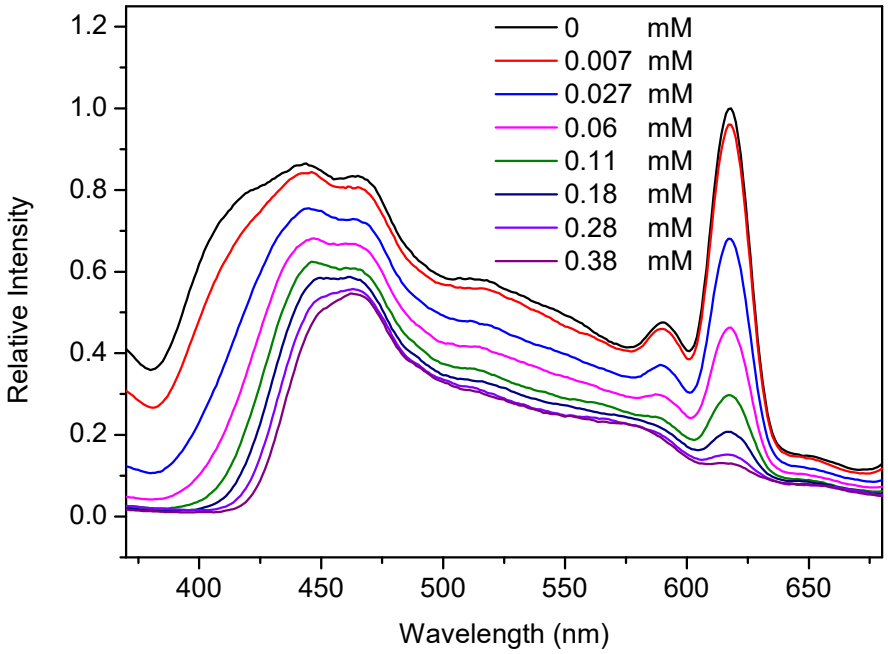

Scheme S1. Molecular structure of selected analysts.

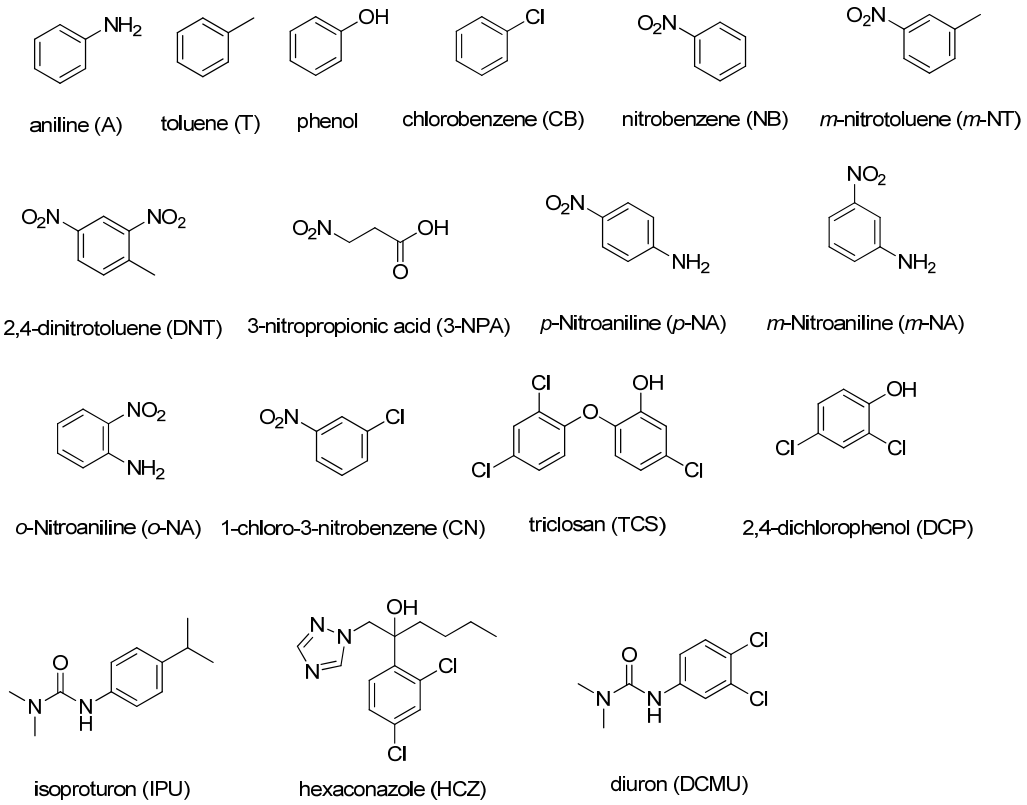

Table S2. Comparison of literature reports for MOFs as sensors of DCN.

Entry	Materials	LOD (μM)	Ref.
1	$[Eu_2(dtztp)(OH)_2(DMF)(H_2O)_{2.5}]\cdot 2H_2O$	7.32	S1
2	$[Zn_2(bpdc)_2(BPyTPE)]$	0.18	S2
3	Mg-APDA	0.2	S3
4	$[Ag(CIP^-)]$	0.18	S4
5	$[Cd_2(HDDB)(bimpy)(NMP)(H_2O)]\cdot 3H_2O$	0.22	S5
6	1a	3.54	S6
7	$[Cd(tptc)_{0.5}(phen)]$	0.1	S7
8	$[Zn_3(DDB)(DPE)]$	0.27	S8
9	$[Cd(tptc)_{0.5}(bpy)]_n$	0.68	S9
10	kgd-M1@ACPs	0.09	S10
11	$[Zn_2(L)_2(TPA)]\cdot 2H_2O$	1.90	S11
12	$\{[Zn(PA^{2-})(dmbpy)](DMF)\}_n$	1.81	S12
13	$[(CH_3)_2NH_2]_2[Li(TCA)]\cdot 0.5DMF\cdot H_2O$	0.62	S13
14	$\{Zn_4(TPOM)(1,4\text{-}NDC)_4\}_n$	0.18	S14
15	$[Cd_3(CBCD)_2(DMA)_4(H_2O)_2]\cdot 10DMA$	0.08	S15
16	$\{[Tb_4(BTDI)_3(H2O)_4]\cdot 4H_2O\cdot solvents\}_n$	0.34	S16
17	$Tb_3(HDDB)(DDB)(H_2O)_6]\cdot H_2O$	0.05	S17
18	$(H_3O)[Zn_2L(H_2O)]\cdot 3NMP\cdot 6H_2O$	2.57	S18
20	Eu@DBDA	0.13	**This work**

Reference:

S1. G.-D. Wang, Y.-Z. Li, W.-J. Shi, B. Zhang, L. Hou and Y.-Y. Wang, *Sens. Actuators B Chem.,* 2021, **331**, 129377.

S2. C.-L. Tao, B. Chen, X.-G. Liu, L.-J. Zhou, X.-L. Zhu, J. Cao, Z.-G. Gu, Z. Zhao, L. Shen and B. Tang, *Chem. Comm.*, 2017, **53**, 9975-9978.

S3. N. Xu, Q.-H. Zhang, B.-S. Hou, Q. Cheng and G.-A. Zhang, *Inorg. Chem.,* 2018, **57**, 13330-13340.

S4. D.-D. Feng, Y.-D. Zhao, X.-Q. Wang, D.-D. Fang, J. Tang, L.-M. Fan and J. Yang, *Dalton Trans.,* 2019, **48**, 10892-10900.

S5. D.-D. Feng, J. Tang, J. Yang, X.-H. Ma, C.-Z. Fan and X.-Q. Wang, *J. Mol. Struct.*, 2020, **1221**, 128841.

S6. M. Hoshi, N. Kaneko, R. Nishiyabu and Y. Kubo, *J. Mater. Chem. C,* 2018, **6**, 11052-11062.

S7. L.-M. Fan, Z.-J. Liu, Y.-J. Zhang, F. Wang, D.-S. Zhao, J.-D. Yang and X.-T. Zhang, *New J. Chem.,* 2019, **43**, 13349-13356.

S8. X.-Q. Wang, D.-D. Feng, J. Tang, Y.-D. Zhao, J. Li, J. Yang, C. K. Kim and F. Su, *Dalton Trans.,* 2019, **48**, 16776-16785.

S9. L.-M. Fan, F. Wang, D.-S. Zhao, X.-H. Sun, H.-T. Chen, H.-W. Wang and X.-T. Zhang, *Spectrochim. Acta A Mol. Biomol. Spectrosc.,* 2020, **239**, 118467.

S10. W.-W. Jia, R.-Q. Fan, J. Zhang, Z.-Q. Geng, P.-X. Li, J.-K. Sun, S. Gai, K. Zhu, X. Jiang and Y.-L. Yang, *Food Chem.,* 2022, **377**, 132054 .

S11. X.-Y. Guo, Z.-P. Dong, F. Zhao, Z.-L. Liu and Y.-Q. Wang, *New J. Chem.*, 2019, **43**, 2353-2361.

S12. H. Kaur, S. Walia, A. Karmakar, V. Krishnan and R. R. Koner, *J. Environ. Chem. Eng.,* 2022, **10**, 106667.

S13. N. Seal, R. Goswami, M. Singh, R. S. Pillai and S. Neogi, *Inorg. Chem. Front.,* 2021, **8**, 296-310.

S14. G. Chakraborty, P. Das and S. K. Mandal, *ACS Appl. Mater. Interfaces,* 2018, **10**, 42406-42416.

S15. N. Xu, Q-H. Zhang and G.-A. Zhang, *Dalton Trans.,* 2019, **48**, 2683-2691.

S16. Y. Li, B.-L. Chai, H. Xu, T.-F. Zheng, J.-L. Chen, S.-J. Liu and H.-R. Wen, *Inorg. Chem. Front.,* 2022, **9**, 1504-1513.

S17. X.-Q. Wang, X.-H. Ma, D.-D. Feng, J. Tang, D. Wu, J. Yang and J.-J. Jiao, *Cryst. Growth Des.,* 2021, **21**, 2889-2897.

S18. L. Di, Z.-Q. Xia, J. Li, Z.-X. Geng, C. Li, Y. Xing and Z.-X. Yang, *RSC Adv.,* 2019, **9**, 38469-38476.